INTERNATIONAL ATOMIC ENERGY AGENCY
UNITED NATIONS EDUCATIONAL, SCIENTIFIC AND CULTURAL ORGANIZATION
INTERNATIONAL CENTRE FOR THEORETICAL PHYSICS
I.C.T.P., P.O. BOX 586, 34100 TRIESTE, ITALY, CABLE: CENTRATOM TRIESTE

H4.SMR/383 - 23

WORKSHOP ON REMOTE SENSING TECHNIQUES WITH APPLICATIONS TO AGRICULTURE, WATER AND WEATHER RESOURCES

(27 February - 21 March 1989)

SATELLITE INVESTIGATION OF CLOUDS AND CLOUD STRUCTURE

V. LEVIZZANI
Istituto FISBAT - C.N.R.
Reparto Nubi e Precipitazioni
Bologna
ITALY

International Centre for Theoretical Physics

Workshop on Remote Sensing Techniques
with Applications to Agriculture

Trieste February 27 - March 21 1989

Satellite investigation of clouds and cloud structure

V. Levizzani

Istituto FISBAT - C.N.R.
Reparto Nubi e Precipitazioni
Bologna, Italy

1. Atmospheric windows for cloud detection from satellite.

People who use whatever kind of satellite imagery for their professional purposes should ask themselves, at least once in a lifetime, the reason why there are so many channels and different satellite sensors. If one does not understand this, he/she will experience a whole set of difficulties in interpreting what comes out of a satellite image.

Meteorological satellites deal with channels centered in the visible, infrared and, for the newest generation of spacecrafts, microwave spectral region (*Houghton et al., 1986; Schott and Henderson-Sellers, 1984*). The reason to use different channels is due to the fact that the objects (clouds) and phoenomena (weather systems) to be detected usually display a great variability in space and time. What we are interested in is not only to obtain nice pictures of clouds, which could come easily from some visible channel alone, but mainly to examine the external and internal complex structure of cloud systems, especially those which fall within the category of precipitation-producers.

The main problem is that an imaging sensor mounted on a spacecraft has to be able to detect low clouds as well as high clouds with, possibly, the same precision. The top of a cloud could be, for example, only 100 m above sea level; in the case of intense thunderstorms, such as the tropical ones, the top of cumulonimbus clouds can reach as high as 17 Km above sea level. In the first case 99% of the atmospheric mass lies between the cloud top and the satellite sensor so that the energy sent by the cloud top will be attenuated by the thick layer of atmospheric molecules in its path to the satellite radiometer. In the second case you are particularly lucky, since only 10% of the atmosphere would be still between cloud top and satellite. In any event, you should always stick to the worst case of having the greatest part of the atmosphere to deal with, namely to attenuate the energy you want to measure.

For this reason you must choose satellite sensors as much as possible within the so-called atmospheric *windows*, which are nothing but those spectral regions where the atmosphere is virtually transparent to the incoming and outcoming radiation

(*Bunting and Hardy, 1984*).This means that in these regions no strong absorption by any atmospheric constituent is present. Fig.1 shows the atmospheric transmittance for a vertical path to space from sea level for six model atmospheres, as calculated by *Selby and McClatchey (1975)* in the region 0.1 to 28 μm.

Just to give the flavour of the complexity of the absorption of solar radiation by the atmosphere in Fig.2 are reported the absorption bands for the two most important absorbers, i.e. water vapor and CO_2 (*Tomasi and Trombetti, 1985*). As it can be seen, the infrared spectrum of solar radiation at the Earth's surface shows a crowded set of water vapor absorption bands, whose intensity gradually increases with wavelength: these bands absorb a great deal of solar radiation and cause a complete black-out within several intervals of the solar spectrum. The most important bands are:

1) α	0.7 - 0.74	μm	(maximum at 0.718 μm);
2) band 0.8 μm	0.796 - 0.847	μm	(maximum at 0.810 μm);
3) ρ,σ,τ	0.87 - 0.99	μm	(maximum at 0.935 μm);
3) Φ	1.08 - 1.20	μm	(maximum at 1.130 μm);
4) Ψ	1.25 - 1.54	μm	(maximum at 1.395 μm);
5) Ω	1.69 - 2.08	μm	(maximum at 1.87 μm);
6) Χ	2.27 - 2.99	μm	(maximum at 2.68 μm);
7) Χ'	2.99 - 3.57	μm	(maximum at 3.2 μm).

Particular attention must be paid to the strong vibro-rotational band indicated as ν_2 which occupies the interval between 4.88 and 8.7 μm with the maximum at 6.27 μm. It is worth mentioning the CO_2 strong band ν_3 centered at 4.257 μm. Many other bands are relative to other minor atmospheric constituents such as O_3, HDO, CH_4, N_2O, CO and others. We will not discuss them as this is outside our purposes and since water vapor and CO_2 already play the most important role in the wavelength region of meteorological satellites.

Another interesting feature is the spectral distribution of the penetration of solar radiation into the atmosphere. Fig.3 shows the wavelength dependence of the altitude at which the spectral intensity of solar radiation along the vertical path is reduced to 1/e (~ 37%) of the extra-terrestrial value.

From what we have seen so far it comes out that satellite

channels are to be chosen within the above-described atmospheric windows, usually with a spectral response narrower than the bandwidth of the window since it is desirable to avoid some molecular absorption bands present in the "wings" of the window.

2. Physical and optical properties of clouds.

Cloud optical properties such as reflectivity or emissivity depend upon cloud physical properties as well as the wavelength of radiation observed by the satellite. It is of capital importance for many applications to be able to distinguish cloud particles from the larger precipitation particles and water particles from ice particles. For example, a water cloud such as a stratocumulus might contain cloud droplets with radii up to 30 μm in total number concentrations of about 300 cm^{-3} and with liquid mass density of 0.3 g m^{-3}. An ice cloud such as a cirrostratus might contain ice particles shaped like hexagonal prisms with mass-equivalent radii of 10-80 μm, number concentrations up to 0.1 cm^{-3} and total ice density up to 0.05 g m^{-3}. Naturally this is only to make it simple since real clouds show a great variability. To summarize in a short sentence we can say that water clouds have many small particles while ice clouds have relatively few but larger particles; however, both water and ice clouds have particle size distributions peaking at small sizes with fewer large particles.

Given the particle sizes and numbers it is possible to calculate the radiation sent by the clouds to the satellite sensor.The calculation starts with the amount of energy scattered, absorbed and emitted by individual particles. The result depends on the refractive index , which varies with wavelength and the water or ice phase of the particle. Moreover, the result is dependent upon the radius of the particle r and the wavelength λ or, better, on the Mie parameter

$$x = \frac{2 \pi r}{\lambda} \qquad (1)$$

Calculations are accurate for water droplets since their spherical shapes are in accordance with Mie theory; results for ice particles are less certain for their shapes are quite irregular.

Another consideration to be made is that weather satellites have a field of view at cloud altitude which is, in the best case, of 1 Km. Hence they sense billions of cloud particles so that multiple scattering theory must be taken into account.

Table 1 shows a summary of calculated cloud optical properties in the assumption that both water and ice clouds are horizontally homogeneous and optically thick or poorly transmitting at short wavelengths.

In the 1.6-1.7, 2.1-2.3 and 3.5-4.0 μm windows, water clouds tend to reflect more than ice clouds so that these bands can be used to distinguish water clouds from ice clouds during daytime. In the 8-13 μm window, both water clouds and ice clouds are poor reflectors but good emitters; therefore the radiance emitted by the clouds can be used to estimate their temperature by means of the Planck function which relates temperature and wavelength to emitted radiance as follows

$$B_\nu(T) = \frac{2h\nu^3}{c^2\left(e^{h\nu/KT} - 1\right)} \qquad (2)$$

where T is the temperature, h=6.6262x10^{-27} erg sec the Planck's constant, ν the frequency, K=1.38062x10^{-16} erg deg^{-1} the Boltzmann's constant, c=2.99793±1x10^{10} cm sec^{-1}. Some ice cloud are optically thin since they transmit a significant amount of energy from beneath the cloud and emit correspondingly less energy from the cloud. The energy sensed by the satellite sensor is not a reliable indicator of the temperature for these cirrus clouds and the clouds usually appear warmer than they should, due to warmer radiances transmitted through the thin ice clouds. Confirmation that these clouds are optically thin is given by the fact that the Sun or Moon is often visible from the ground through these clouds.

At the microwave windows listed in Table 1, water clouds also differ from ice clouds. At these frequencies, water clouds are

partial absorbers of radiation while ice clouds are nearly transparent. Water clouds with raindrops and substantial water content stand out as warm regions against the cold background of oceans, which are poor emitters at these frequencies. Ice particles will scatter microwave so that ice clouds may act as reflectors at the shorter wavelengths. However, looking down from a satellite there is practically no energy from space to be reflected back to the satellite and the Earth's surface or water clouds can usually be seen through the ice clouds. Land backgrounds have emissivities in the range of 0.75 to 0.95 in the microwave region; these are much higher than for oceans. In contrast, the emissivities for radiation at 8-13 μm are close to 1.0. Consequently, in the microwave region, neither water clouds nor ice clouds contrast with land backgrounds unless the water clouds contain ample raindrops.

The microwave windows also differ from the other windows since the radiation sensed at the satellite may be highly polarized. As a result, microwave imagers have been designed to scan conically so that the angle of incidence to the Earth's surface remains constant during the scan. The horizontal as well as vertical polarizations are measured for each window which provides additional information on the medium being observed.

3. The problem of cloudy images interpretation.

A skilled meteorologist, looking at a satellite image and only using his experience, is able to both identify and characterize clouds. Satellite images display spatial features of clouds and multispectral features if more than one channel is available. The human eye and brain have developed an extremely talented system for pattern recognition which is very successful in the interpretation of images. By simply looking at a satellite image your eye can readily adjust to different backgrounds, such as forest, farmland, mountains, oceans and coastlines, which have different reflectivities at solar wavelengths and often have different temperatures at thermal wavelengths; in an automated

approach, if you are not careful, these varying backgrounds may be confused with clouds. Recognizing geographical features tells the analist that clouds are not presumably present in the image, but in some particular case the results are not so sure. As a revealing example we could think about narrow valleys in the mountains filled up with snow while the peaks are bare soil: if you have a scattered cloud cover whose top temperature is comparable with that of the snow on the surface, the job of automatically separate snow and clouds is going to be quite complicate!

It is, then, of great importance to make the best use of satellite multispectral information in order to separate clouds from other features and to classify different cloud types. In the following we will examine two of the most up-to-date cloud classification methods, the first being based upon geostationary satellite data, and the second on polar orbiting multi-channel data.

4. Cloud classification on METEOSAT imagery.

There is a great need for automatic cloud classification (nephanalysis) on satellite imagery for research in mesoscale meteorology and numerical modeling, but especially as a specific aide to very-short-range weather forecasts (*nowcasting*).

Nowcasting procedures heavily rely upon geostationary satellite imagery because of its spatial and temporal coverage of the areas of interest: both genesys and evolution of precipitating systems are detected and followed every half an hour so that the meteorologist has a precise idea of the behaviour of the cloud systems he is trying to predict. The resolution of the satellite imagery makes it possible to issue forecasts which are tailored to the scale and time of the user, among whom one of the most important is agriculture (*Prodi and Levissani, 1986*).

The most recent technique of cloud classification applied to METEOSAT imagery is the one developed by *Desbois et al.* (*1982*) which refers to the radiative properties of the clouds as a basis

for defining classes in the two- or three-dimensional space of the channels.

The method is based upon dinamic clustering of images in the three channels of the METEOSAT (visible, infrared and water vapor), i.e. it separates classes on three-dimensional histograms. What is of capital importance is that no a priori training set is used, that is no previous classification of the points of the histogram has to exist. It is well known that in simple cases two-dimensional histograms show that every well-defined cloud type can be associated with a specified spectral signature on the diagram. Fig.4 reports an example of such a bidimensional histogram. Although general cases of histograms for real meteorological situations are not so simple, it can be reasonably assumed that every kind of clouds is represented in the spectral domain by a compact subset of the projection of the image segment in this domain. This essentially means that all the points of the same subset are close to each other, according to the Euclidean distance, and all the subsets are disjoint.

The method can be summarized as follows:

a) A given number of N classes is chosen.
b) A set of F points is then chosen randomly for each class (this set is called the Kernel of the class).
c) For each kernel the center of gravity and the variance are calculated.
d) Classes are constructed: each point is affected to the class of which the center of gravity of the kernel is closest. During this process, if the number of elements of one class becomes very small, the class is suppressed.
e) The center of gravity and the variance of the classes are calculated again.
f) New kernels of F points are defined again.
g) A new iteration is started form c).

Iterations are carried out until the distance between the centers of gravity of a class and the corresponding kernel remains constant.

The method can be applied to as many dimensions as are needed (1 to n channels). The point to use more than one channel is to extract from multi-channel imagery more information than is

included in only one spectral band. Clusters obtained with different combinations of many spectral channels reveal fine structured features which allow a precise identification of cloud types along with the separation of uninteresting classes (meteorologically speaking) like land, sea and sunglints among others.

In Fig.5a-c the first result of Institute FISBAT satellite cloud classification scheme is reported. Fig.5a and 5b show the uni-dimensional histograms of the visible and infrared channel of METEOSAT for a case of a frontal passage over Italy on November 22 1987. As it can be noticed already from the unidimensional histograms two big classes are evidenced: one is dark/warm and the other bright/cold. When considering the bi-dimensional histogram resulting from a unification of the two uni-dimensional (see Fig.5c) the classes appear as clusters in the Vis-Ir plane. Two clusters are present in the lower-left corner and represent, respectively from left to right, the two big categories of land and sea. The other recognizable cluster is the one which shows up in the central-upper part of the graph: this is the most interesting class since reveals the presence of relatively bright and cold objects in the image, essentially the clouds of the precipitating system. One more step further (actually under investigation at Institute FISBAT) would be to include a classification of the type of clouds (most of all cumulonimbus, nimbostratus, stratocumulus) directly associated to precipitation. With this in mind the water vapor channel is being taken also into account as to ensure another information source especially for high-level clouds delineation, such as cold and thin veils of cirrus.

5. Cloud analysis with polar orbiting satellites.

Another approach that has been followed to operationally identify and classify clouds is the analysis of polar orbiting satellite imagery. The reasons for this approach are of two orders: 1) multispectral analysis using the higher number of

spectral channels of these satellites with respect of geostationary satellites, and 2) cloud analysis in areas of the earth not properly covered by geostationary satellites (e.g. high latitudes areas where the image's curvature is very high).

In Table 2 are reported the main channels of the polar orbiting satellites of the NOAA-Series with their most important uses.

The most advanced of these methods has been developed by *Liljas (1984)* and is based upon imagery from the AVHRR (Advanced Very High Resolution Radiometer) mounted on the NOAA-Series satellites. The idea underlying the method is once more the box classification that has been described for the case of METEOSAT data in the previous chapter. What is new is the very abundant set of information that comes out of the different channels and the ambition to include cloud texture analysis.

The different channels of the satellite in the visible-infrared spectrum are used to construct bi-dimensional histograms of the type already described above, but making use of the enhanced features of the polar orbiting satellites, such as the presence of the infrared channel at 3.7 μm wavelength (*Liljas, 1986*). In fact, simple box classification schemes based only on visible and near infrared (11 μm) channels are sometimes not able to classify imagery at low sun elevation angles in winter and they fail during the night for obvious reasons. Other limitations are sunglints in the morning and evening passages during spring and fall: sunglints are classified as stratus, fog or mist. Cirrus clouds over lower clouds are sometimes classified as nimbostratus, which is highly dangerous in automatic precipitation analysis. Snow has signatures in these bands which is too close to that of different clouds.

Channel 3 of NOAA polar orbiting satellites (3.7 μm) produces a quite complex kind of imagery during the day since it includes both reflected solar radiation and emitted terrestrial radiation. The radiative properties of water droplet and ice clouds are related by the equation (*Hunt, 1973*)

$$\varepsilon + re + tr = 1 \qquad (3)$$

where ε, re and tr are the emissivity, reflectivity and

transmissivity of the cloud layer, respectively. The following facts are to be considered:

a) an increase of the particles sizes has the effect of increasing the transmissivity and emissivity and decreasing the reflectivity of the cloud layer;

b) at infrared windows water droplet and ice clouds do not behave like blackbody radiators;

c) the emissivities of the ice clouds are less than the corresponding for water droplet clouds as a consequence of their lower water content;

d) at 3.9 μm window the emissivity of a cloud layer is less than its value at 8.5-13 μm window; there is a large contribution to the emergent field of radiation reflected by the cloud top at the shorter wavelengths that is absent for the 8.5-13 μm radiances;

e) in the 8.5-13 μm window the emergent radiance is dominated by the emitted radiation from the cloud layer.

For optically thick clouds the transmissivity vanishes and equation (3) simplifies to

$$r\varepsilon + \varepsilon = 1 \qquad (4)$$

Land, water and snow surfaces have reflectivities close to 0 in the window around 3.7 μm.

To simplify the interpretation of the daytime 3.7 μm imagery *Liljas (1986)* subtracts from it the emitted radiation component in the form of the 11 μm channel radiance: then new images are constructed subtracting channel 4 from channel 3. In the new images the dominant features result from reflected solar radiance at 3.7 μm.

Fig.6 shows a result of the described groupings of different reflected surfaces in the two-dimensionale intensity space of channel 3-channel 4 and channel 1; the bands are normalized by dividing by sin(α), where α is the sun elevation angle. The most interesting features are the following:

a) sunglints are separated from stratus, fog and land;

b) snow is well separated from clouds with the same reflectivity at visible wavelengths and temperature;

c) cumulonimbus and nimbostratus clouds have a weaker reflectivity

relative to other cloudsand the reflectivity in channel 1; developing cumulonimbus appear warmer in channel 3 than the decaying ones;

d) cirrus clouds appear relatively warm in channel 3, especially thin cirrus over low level clouds;

e) mist has a significant reflectivity in channel 3.

6. Conclusions.

Satellite imagery is actually the best source of information for the identification of different classes of mesoscale cloud systems and mesoscale structure of synoptic scale systems.

Colour images, after the classification process, give a good indication of cloud structure in various systems, their stage of development and also of the stability of the atmosphere. For example, stratocumulus, small cumulus and daytime fog or stratus indicate stable conditions in the lower troposphere. Groups or lines of large cumulus elements in the morning indicate humid and unstable conditions at the early stage of a mesoscale system leading to cumulonimbus and thunder. Cumulus growing into cumulonimbus shows where a mesoscale convective system is under development. A cloud system consisting mainly of cirrostratus or altocumulus generated from cumulonimbus indicates the final and decaying phase of the life cycle of a mesoscale convective system.

Applications to operational weather forecasting is greatly recommended especially in the framework of very short range forecasting or *nowcasting*. The forecaster is given the powerful capabilities of multispectral analysis which provide him an additional "eye" to sense cloud systems, enhancing the conventional methods by some order of magnitude.

Response	λ	Water cloud	Ice cloud	Ice cloud over rain
Reflectivity of sunlight when the Sun is overhead	0.7 μm	0.80	0.80	0.80
	1.7 μm	0.70	0.20	0.20
	2.1 μm	0.50	0.05	0.05
	3.7 μm	0.30	0.10	0.10
Emissivity for thermal radiation	3.7 μm	0.70	0.90	0.90
	11.5 μm	0.95	0.95	0.95
Temperature increase, due to clouds over an ocean (K)	0.32 cm (94 GHz)	24	0	41
	0.81 cm (37 GHz)	12	0	30
	1.55 cm (19 GHz)	3	0	11

Table 1. Representative cloud responses in atmospheric windows. These numbers vary with cloud depth, width and particle size. Only tipical values are given: the radiation calculations assume that clouds are horizontally extensive and that radiation sensors are looking straight down.

Channel	Wavelength (μm)	Primary use
1	0.58 - 0.68	Daytime cloud and surface mapping
2	0.725 - 1.10	Surface water delineation
3	3.55 - 3.93	Sea surface temperature (SST), night time cloud mapping
4	10.5 - 11.5	SST, day/night cloud mapping
5	11.5 - 12.5	SST

Table 2. NOAA AVHRR channels.

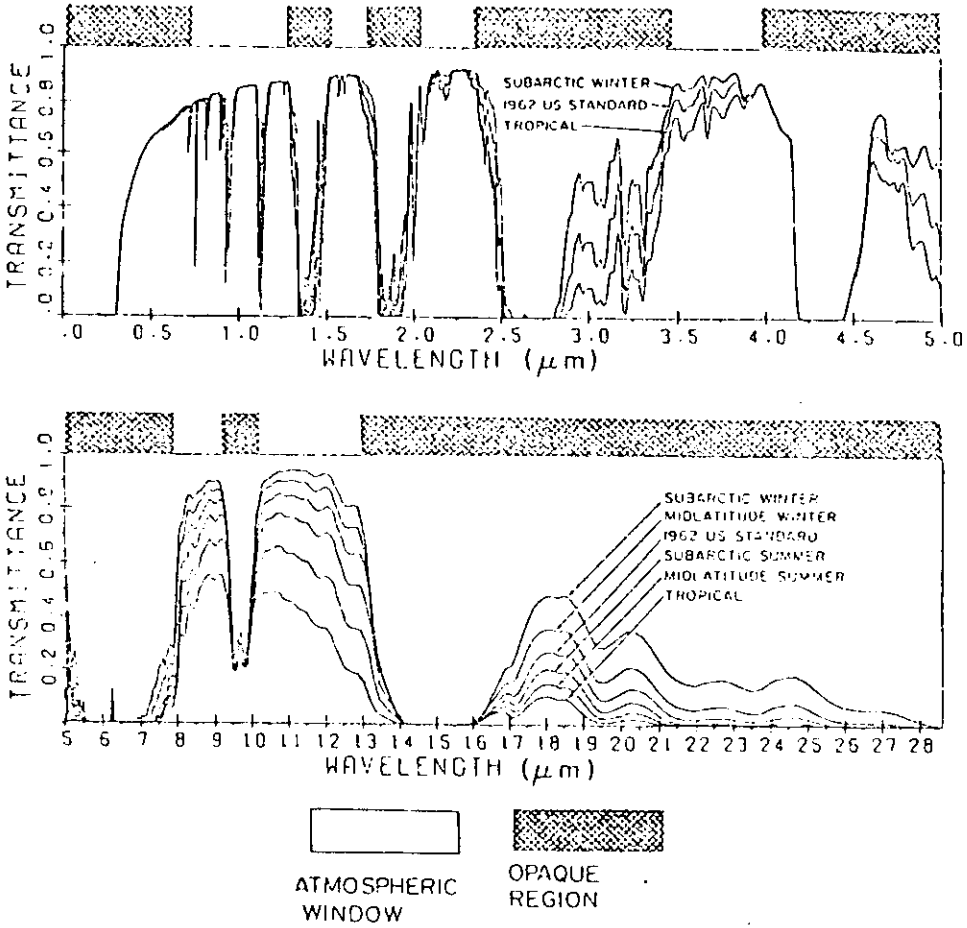

Fig.1 Atmospheric transmittance for a vertical path to space from six model atmospheres, calculated by *Selby and McClatchey (1975)*. Atmospheric windows used for cloud detection are distinguished from more opaque wavelengths.

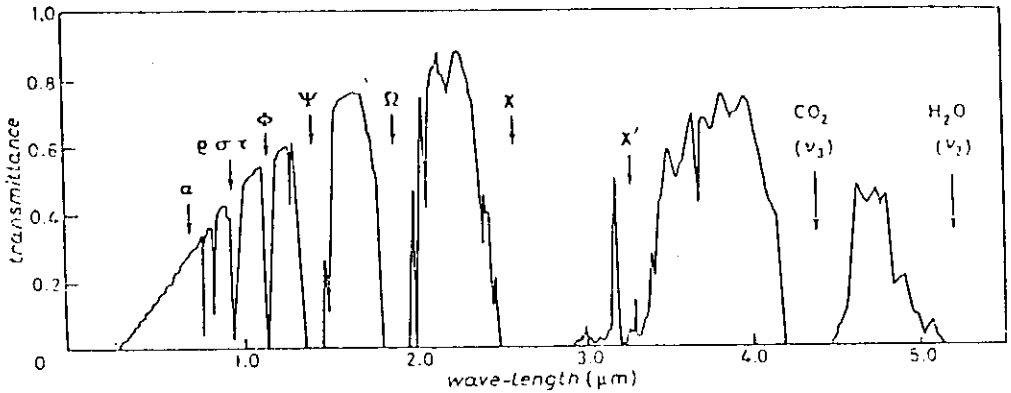

Fig.2 Atmospheric transmittance spectrum from the visible to the middle infrared region as calculated for the US 1962 Standard Atmosphere with visual range of 23 Km at the Earth's surface (*Tomasi and Trombetti, 1985*). The various absorption bands due to water vapor and carbon dioxide are indicated by greek letters.

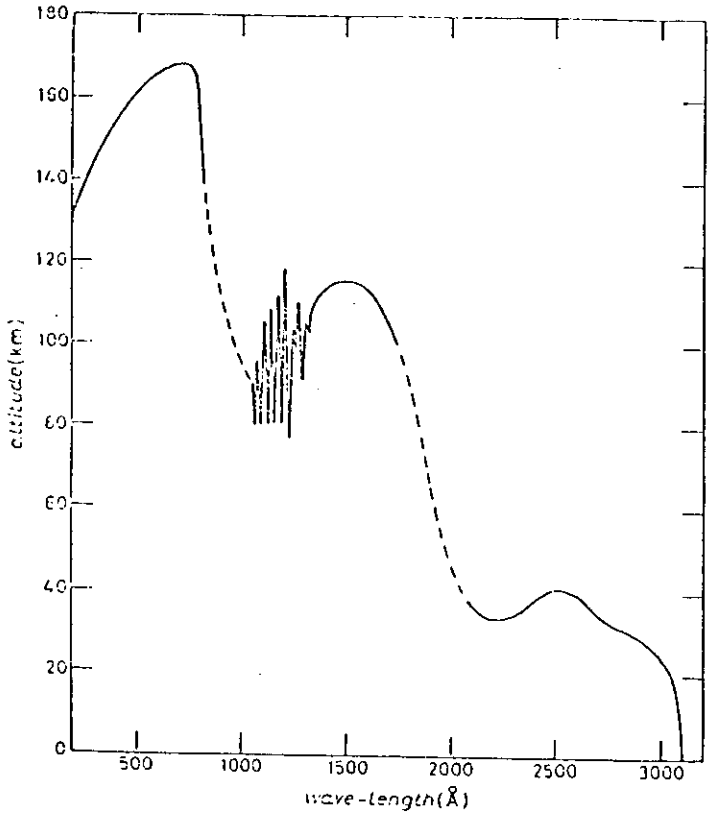

Fig.3 Spectral distribution curve representing the penetration of solar radiation into the atmosphere (*Tomasi and Trombetti, 1985*). The curve gives the altitude at which the intensity of the incoming solar radiation along the vertical path is reduced to 1/e of the value outside the terrestrial atmosphere.

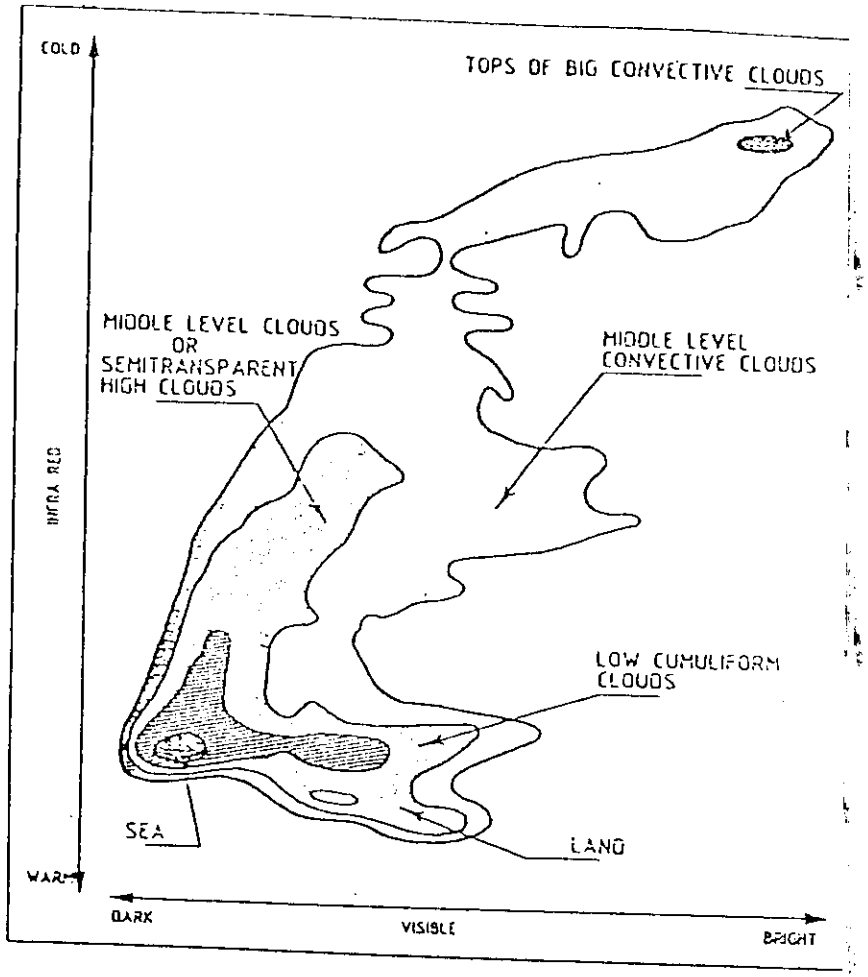

Fig.4 VIS-IR METEOSAT bi-dimensional histogram of cloud types (*Desbois et al. 1982*).

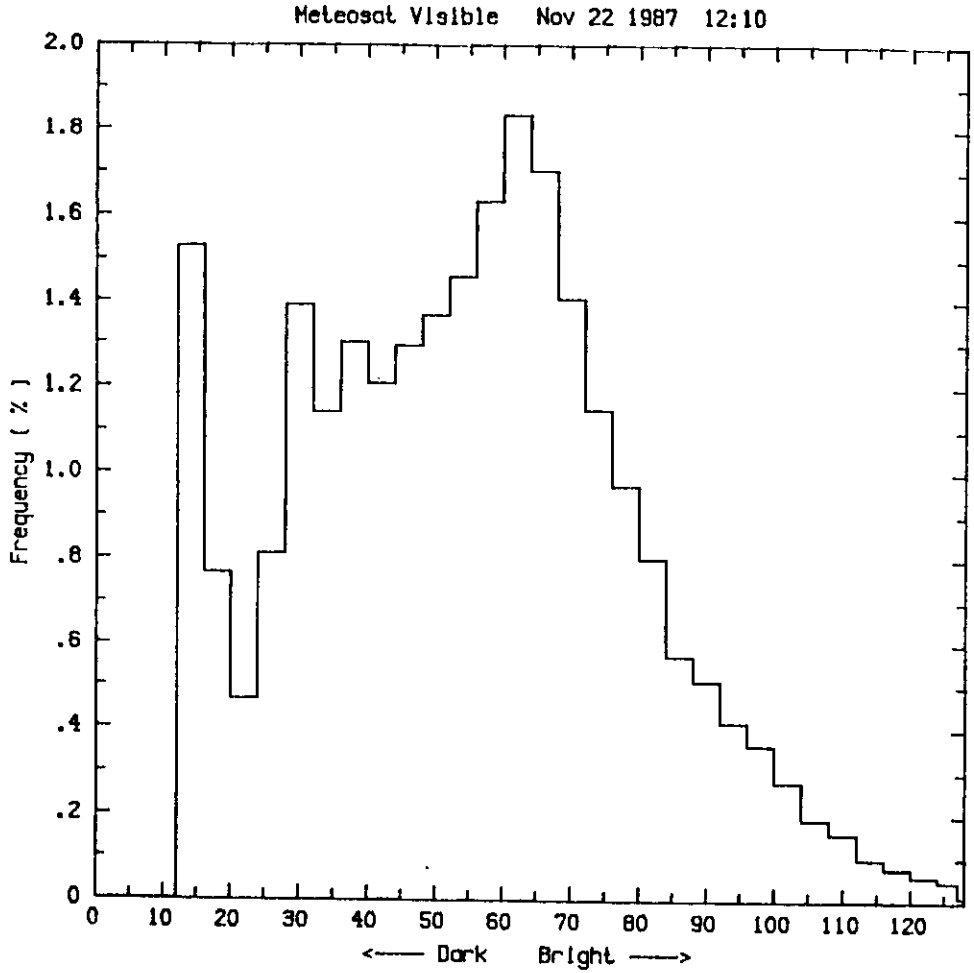

Fig.5a Histogram of the visible channel of METEOSAT for an image relative to a precipitating event on Nov 22 1987; the image was 396 x 202 pixels, covering the whole Italy and northern mediterranean area.

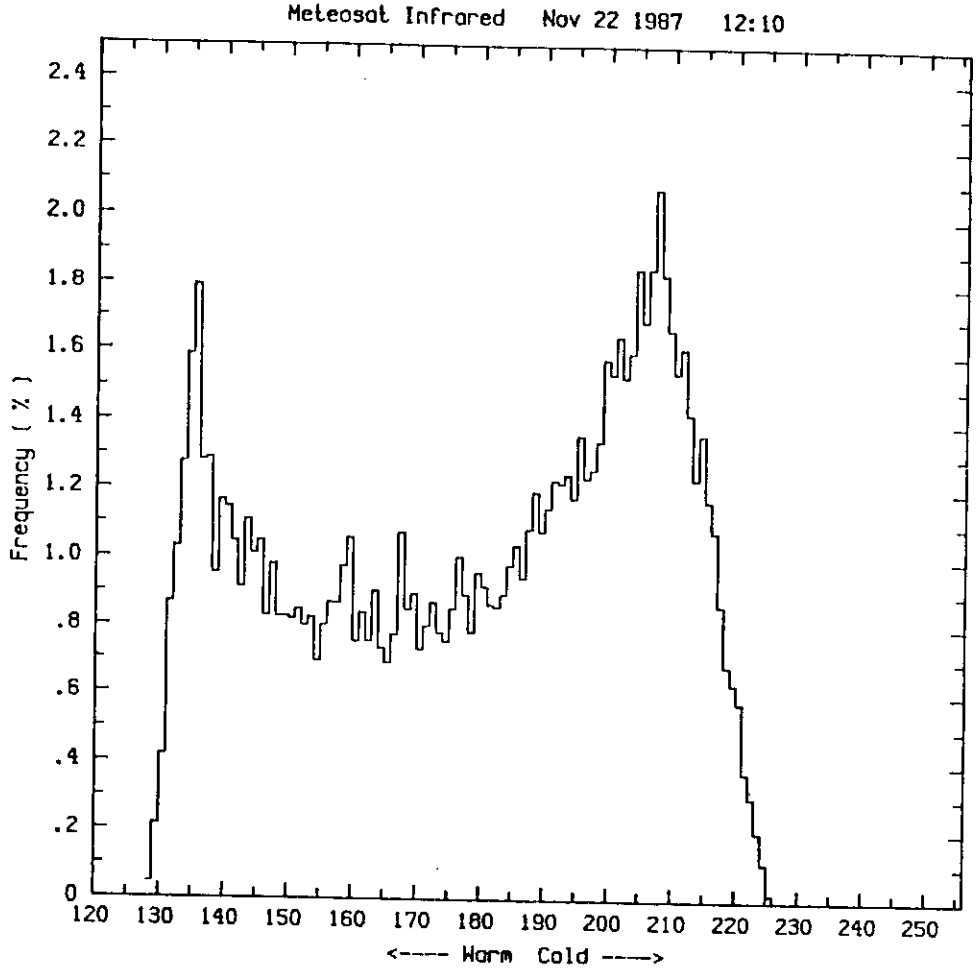

Fig.5b Same as in Fig.5a except for METEOSAT thermal infrared channel.

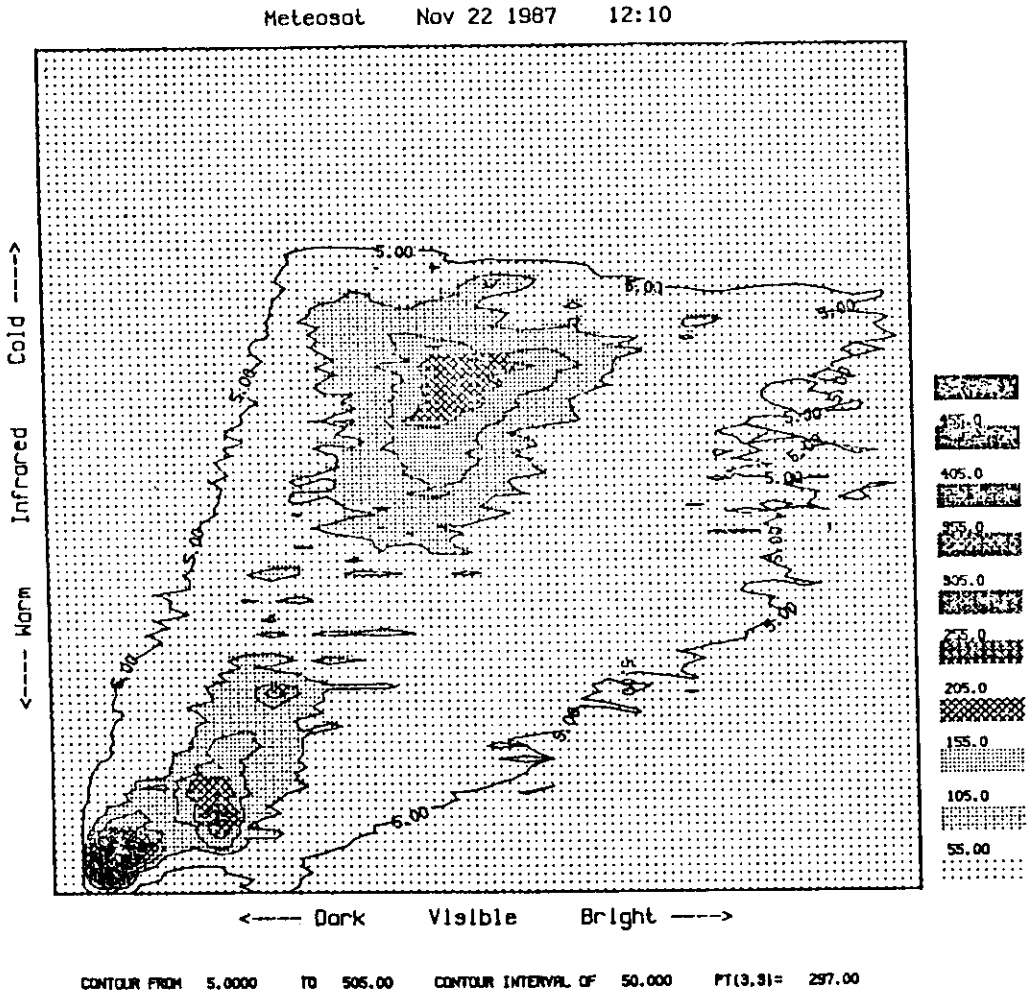

Fig.5c Bi-dimensional histogram derived for the same case as in Fig.5a-b. Values are relative to the number of pixels present in each class. Three main classes are evidenced: land (lower-left corner), sea (on the right of the previous class) and high level precipitating clouds (center-upper part).

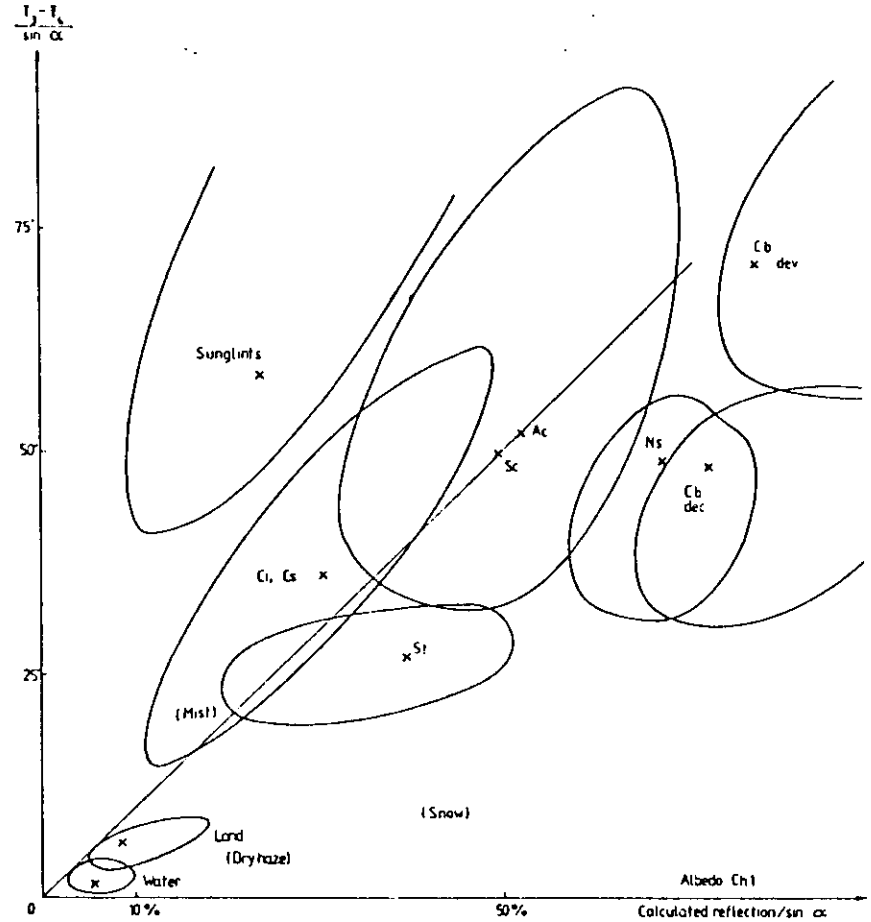

Fig.6 Multispectral cloud classification using polar orbiting NOAA-Series satellite imagery (*Liljas, 1984*). Reflection of channel 3 - channel 4 is displayed in ordinate and reflection from channel 1 in abscissa; the values are normalized dividing by sin(α) for an overhead sun.

References.

Bunting,J.T. and K.R.Hardy, 1984. Cloud identification and characterization from satellite. In *Satellite sensing of a cloudy atmosphere-Observing the third planet*, A.Henderson-Sellers Ed., Taylor & Francis, London, 203-240.

Desbois,M., G.Sese and G.Szejwach, 1982. Automatic classification of clouds on METEOSAT imagery: application to high-level clouds. *J.Appl.Meteor.*, 21, 401-412.

Houghton,J.T., F.W.Taylor and C.D.Rodgers, 1986. *Remote sounding of atmospheres*, Cambridge Univ. Press, Cambridge, 343 pp.

Hunt,G.E., 1973. Radiative properties of terrestrial clouds at visible and infrared thermal window wavelengths. *Quarterly J. Royal Meteor. Soc.*, 99, 346-369.

Liljas,E., 1984. *Processed satellite imageries for operational forecasting.* Report Swedish Meteorological and Hydrological Institute, Norrköping, Sweden, 43 pp.

Liljas,E., 1986. *Use of the AVHRR 3.7 micrometer channel in multispectral cloud classification.* SMHI Promis-Rapporter, nr.2, Swedish Meteorological and Hydrological Institute, Norrköping, Sweden, 23 pp.

Prodi,F. and V.Levizzani, 1986. Meteorological nowcasting through satellite and radar image processing. In *The Records of the International Conference on the Arno Project*, Florence, 24-25 Nov.

Schott,J.R. and A.Henderson-Sellers, 1984. Radiation, The atmosphere and satellite sensors. In *Satellite sensing of a cloudy atmosphere-Observing the third planet*, A.Henderson-Sellers Ed., Taylor & Francis, London, 45-89.

Selby,J.E.A. and R.A.McClatchey, 1975. *Air Force Geophysical Laboratory Technical Report No. 75-0255*, Hanscom, Mass. 01731, U.S.A.

Tomasi,C. and F.Trombetti, 1985. Absorption and emission by minor atmospheric gases in the radiation balance of the Earth. *Il Nuovo Cimento, C*, 8, n.2, 1-89.